Atmos. Chem. Phys., 18, 799–813, 2018
https://doi.org/10.5194/acp-18-799-2018

Atmospheric Chemistry and Physics
Open Access
EGU

Emission of nitrous acid from soil and biological soil crusts represents an important source of HONO in the remote atmosphere in Cyprus

Hannah Meusel[1], Alexandra Tamm[1], Uwe Kuhn[1], Dianming Wu[1,a], Anna Lena Leifke[1], Sabine Fiedler[2], Nina Ruckteschler[1], Petya Yordanova[1], Naama Lang-Yona[1], Mira Pöhlker[1], Jos Lelieveld[3,4], Thorsten Hoffmann[5], Ulrich Pöschl[1], Hang Su[6,1], Bettina Weber[1], and Yafang Cheng[1,6]

[1]Max Planck Institute for Chemistry, Multiphase Chemistry Department, Mainz, Germany
[2]Johannes Gutenberg University, Institute for Geography, Mainz, Germany
[3]Max Planck Institute for Chemistry, Atmospheric Chemistry Department, Mainz, Germany
[4]The Cyprus Institute, Nicosia, Cyprus
[5]Johannes Gutenberg University, Institute for Inorganic and Analytical Chemistry, Mainz, Germany
[6]Institute for Environmental and Climate Research, Jinan University, Guangzhou, China
[a]now at: School of Geographic Sciences, East China Normal University, Shanghai, China

Correspondence: Hang Su (h.su@mpic.de) and Bettina Weber (b.weber@mpic.de)

Received: 20 April 2017 – Discussion started: 2 May 2017
Revised: 27 November 2017 – Accepted: 9 December 2017 – Published: 23 January 2018

Abstract. Soil and biological soil crusts can emit nitrous acid (HONO) and nitric oxide (NO). The terrestrial ground surface in arid and semiarid regions is anticipated to play an important role in the local atmospheric HONO budget, deemed to represent one of the unaccounted-for HONO sources frequently observed in field studies. In this study HONO and NO emissions from a representative variety of soil and biological soil crust samples from the Mediterranean island Cyprus were investigated under controlled laboratory conditions. A wide range of fluxes was observed, ranging from 0.6 to 264 ng m^{-2} s^{-1} HONO-N at optimal soil water content (20–30 % of water holding capacity, WHC). Maximum NO-N fluxes at this WHC were lower (0.8–121 ng m^{-2} s^{-1}). The highest emissions of both reactive nitrogen species were found from bare soil, followed by light and dark cyanobacteria-dominated biological soil crusts (biocrusts), correlating well with the sample nutrient levels (nitrite and nitrate). Extrapolations of lab-based HONO emission studies agree well with the unaccounted-for HONO source derived previously for the extensive CYPHEX field campaign, i.e., emissions from soil and biocrusts may essentially close the Cyprus HONO budget.

1 Introduction

Nitrous acid (HONO) plays an important role in tropospheric chemistry, as it is one of the major precursors of the hydroxyl (OH) radical, which determines the oxidizing capacity of the atmosphere. In the early morning, HONO photolysis has been shown to contribute up to 30 % to the local OH budget (Alicke et al., 2002; Kleffmann et al., 2005; Ren et al., 2003, 2006; Meusel et al., 2016). Currently, the HONO formation processes, especially during daytime, are still not fully understood. Recent ground-based field measurements showed unexpectedly high daytime concentrations of HONO, which could not be solely explained by atmospheric gas-phase reactions (R1–R3) (Kleffmann et al., 2003, 2005; Su et al., 2008a; Sörgel et al., 2011a; Su et al., 2011; Michoud et al., 2014; Czader et al., 2012; Wong et al., 2013; Tang et al., 2015; Oswald et al., 2015, Meusel et al., 2016).

$$\mathrm{OH + NO \rightarrow HONO} \quad \text{(R1)}$$

$$\mathrm{HONO} \xrightarrow{h\nu\,(300-405\,\mathrm{nm})} \mathrm{OH + NO} \quad \text{(R2)}$$

$$\mathrm{HONO + OH \rightarrow NO_2 + H_2O} \quad \text{(R3)}$$

Several studies have shown that HONO can be heterogeneously formed from NO_2 on a variety of surfaces, e.g., soot,

humic acid, minerals, proteins and organically coated particles (Ammann et al., 1998; Arens et al., 2001; Aubin et al., 2007; Bröske et al., 2003; Han et al., 2016; Kalberer et al., 1999; Kleffmann et al., 1999; Kleffmann and Wiesen, 2005; Lelièvre et al., 2004; Kinugawa et al., 2011; Liu et al., 2015; Wang et al., 2003; Yabushita et al., 2009; Meusel et al., 2017). Light can activate some of these surfaces (humic acid, proteins and other organic compounds, titanium dioxide, soot), which enhances NO_2 uptake and HONO production (George et al., 2005; Langridge et al., 2009; Monge et al., 2010; Ndour et al., 2008; Ramazan et al., 2004; Stemmler et al., 2007; Kebede et al., 2013; Meusel et al., 2017). However, NO_2 uptake coefficients and the ambient aerosol surface areas for heterogeneous reactions of NO_2 were nevertheless frequently found to be too low to account for the observed HONO production rates (Stemmler et al., 2007; Sarwar et al., 2008; Zhang et al., 2016). In addition to the heterogeneous NO_2 reaction, Bejan et al. (2006) observed HONO formation during irradiation of nitrophenols. Photolysis of nitrate or nitric acid generates HONO as well (Baergen and Donaldson, 2013; Scharko et al., 2014; Zhou et al., 2003, 2011). Contrary to the detected missing HONO source near the ground, recent airborne measurements (500–1200 m a.g.l., above ground level) observed HONO concentrations, which could be explained by gas-phase reactions only (Li et al., 2014; Neuman et al., 2016). However, vertical gradient studies showed higher HONO concentrations near the ground than in higher altitudes, indicating a ground level source (Harrison and Kitto, 1994; Kleffmann et al., 2003; Ren et al., 2011; Stutz et al., 2002; VandenBoer et al., 2013; Villena et al., 2011; Zhou et al., 2011; Wong et al., 2012, 2013; Vogel et al., 2003; Zhang et al., 2009; Young et al., 2012). This is supported by gas exchange studies showing that HONO and NO can be emitted from (natural) soil and biological soil crusts (biocrusts, BSCs), even without applying atmospheric NO_2 (Su et al., 2011; Oswald et al., 2013; Mamtimin et al., 2016; Weber et al., 2015; Meixner and Yang, 2006). HONO and NO can be formed during biological processes (nitrification and denitrification; Pilegaard, 2013), in which NH_3 or NH_4^+ is oxidized stepwise or NO_3^- is reduced (Fig. 1). Depending on soil pH and according to Henry's law, soil nitrite (NO_2^-) can be converted into gaseous HONO. It was found that sterilized soil emits lower amounts of reactive nitrogen than natural soil (Oswald et al., 2013; Weber et al., 2015).

Biocrusts grow within the uppermost millimeters to centimeters of soil in arid and semiarid ecosystems. They are composed of photoautotrophic cyanobacteria, algae, lichens, and bryophytes, growing together with heterotrophic bacteria, fungi and archaea in varying proportions (Belnap et al., 2016). Depending on the dominating photoautotrophs, cyanobacteria-dominated biocrusts with an initial thin light-colored and well-developed dark type, cyanolichen- and chlorolichen-dominated biocrusts with lichens comprising cyanobacteria or green algae as photobionts, and bryophyte-dominated biocrusts are distinguished (Büdel et al., 2009). Many free-living cyanobacteria but also those in symbiosis with fungi (forming lichens) and vascular plants can fix atmospheric nitrogen N_2 and convert it into ammonia (Cleveland et al., 1999; Belnap, 2002; Herridge et al., 2008; Barger et al., 2016). Globally it has been estimated that 100–290 Tg (N) yr^{-1} is fixed biologically (Cleveland et al., 1999), of which 49 Tg yr^{-1} (17–49 %) is fixed by cryptogamic covers, which comprise biocrusts, but also other microbially dominated biomes, like lichen and bryophyte communities occurring on soil, rocks and plants in boreal and tropical regions (Elbert et al., 2012). Studies have suggested that nitrogen cycling in soil (N_2 fixation, nitrification, denitrification) and hence reactive nitrogen emission (NO, N_2O, HONO) is often enhanced by well-established biocrusts, especially by dark cyanobacteria (Cleveland et al., 1999; Elbert et al., 2012; Belnap, 2002; Barger et al., 2013; Johnson et al., 2005; Abed et al., 2013; Strauss et al., 2012; Weber et al., 2015). However, much of the molecular biology and chemistry that is important for atmosphere–land interactions likely occurs just below the crust (that is visible at the surface).

In Cyprus, an island in the semiarid eastern Mediterranean area, biocrusts ubiquitously cover ground surfaces and hence can be anticipated to play an important role in the local HONO budget. In the CYPHEX (CYprus PHotochemical EXperiment) campaign in 2014 the observed diel cycles of HONO ambient air concentrations revealed strong unaccounted-for sources of HONO and NO that were well correlated with each other (Meusel et al., 2016). With low NO_2 concentrations and high $HONO / NO_x$ ratios, direct emissions from combustion and heterogeneous reactions of NO_2 could be excluded as significant HONO sources, leaving emissions from soil and the respective surface cover to be the most plausible common source for both nitrogen species (Meusel et al., 2016).

In the present study we have measured HONO and NO fluxes from soil and biocrust samples from Cyprus by means of a dynamic chamber system. The aim of this study was to characterize and quantify direct trace gas emissions and demonstrate their impact on the atmospheric chemistry in the remote coastal environment of Cyprus.

2 Methods

2.1 Sampling

Bare soil and biocrust samples were collected on 27 April 2016 on the southern-southeastern side of the military station in Ineia, Cyprus (34.9638° N, 32.3778° E), where the CYPHEX campaign took place in 2014. It is a rural site about 600 m a.s.l. (above sea level) and approximately 5–8 km from the coast and is surrounded by typical Mediterranean vegetation (olive and pine trees; small shrubs like *Pistacia lentiscus, Sacopoterium spinosum* and *Inula*

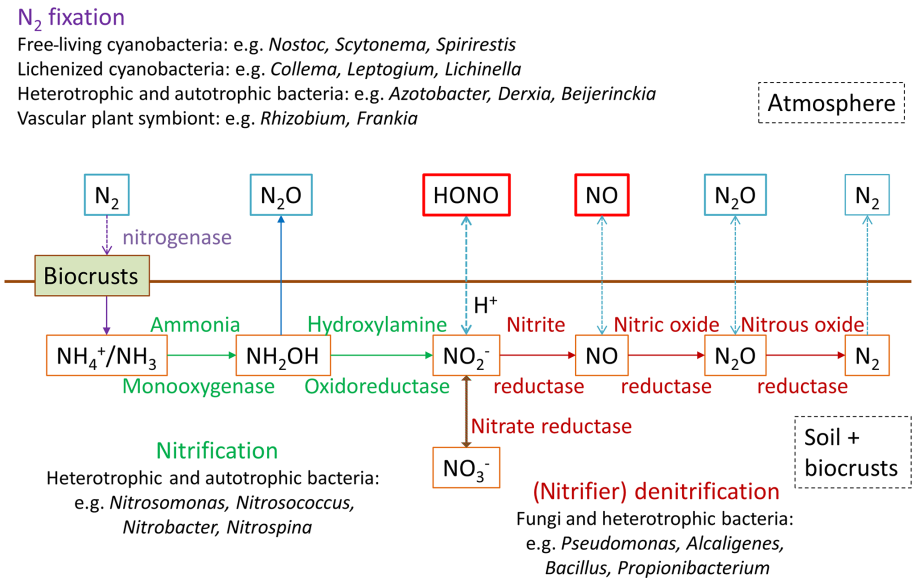

Figure 1. Nitrogen cycle at the atmosphere and pedosphere–biosphere interface including nitrogen fixation, nitrification, denitrification and emission. Enzymes and organisms involved are specified.

viscosa). More details about the site can be found in Meusel et al. (2016).

In an area of about 8580 m^2 (southern-southeastern direction of the station) 50 grids (25 × 25 cm) were placed at randomly selected spots for systematic ground cover assessment. At each grid point occurrence of nine types of surface cover (i.e., light and dark cyanobacteria-, chlorolichen-, cyanolichen-, and moss-dominated biocrust; bare soil; stone; litter; vascular vegetation/shrub) were assigned and quantified. Spatially independent replicate samples of light cyanobacteria-dominated biocrusts (light BSC), dark cyanobacteria-dominated biocrusts with cyanolichens (dark BSC), chlorolichen-dominated biocrusts (chlorolichen BSC I, chlorolichen BSC II), moss-dominated biocrusts (moss BSC) and of bare soil were collected (Fig. S1 in the Supplement). Each sample was collected in dry state in a plastic petri dish (diameter 5.5. cm, height 1 cm), sealed and stored in the dark at room temperature until further analysis (storage time less than 15 weeks). Storage of biocrust samples under dry and dark conditions at room temperature is the most widely spread method and has been used in many other studies on N cycling in which samples have been stored even up to 6 months before measurements were performed (Abed et al., 2013; Strauss et al., 2012; Johnson et al., 2007; Brankatschk et al., 2013).

In total 43 samples were collected (Table 1) of which 18 samples, i.e., three replicates of each HONO-emitting surface cover type, were used directly (upfront) for nutrient analysis, while all others were first used for trace gas exchange measurements prior to nutrient and chlorophyll content analysis.

2.2 Meteorological data

During CYPHEX the meteorological parameters were measured at about 5 m a.g.l., considered not representative for the microhabitat of the soil ground surface. Hence, we placed three humidity (and temperature) sensors (HOBO Pro v2) just on top of the soil surface about 4 weeks prior to sample collection. Reference meteorological data (air temperature, humidity and precipitation) from Paphos airport (about 20 km south of the sample area, 12 m a.s.l.) and Prodromos (about 40 km east of the sampling area, 1380 m a.s.l.) during the sampling period as well as the precipitation data from the last 4 years (2013–2016) were provided by the Department of Meteorology, Cyprus (http://www.moa.gov.cy/moa/ms/ms.nsf/DMLmeteo_reports_en/MLmeteo_reports_en?opendocument; last access: December 2016).

2.3 Soil characteristics: nutrient, chlorophyll and pH

Soil characteristics (nutrient, pH) have an effect on soil emission, e.g., higher nutrient level and lower pH would enhance emission according to Henry's law (Su et al., 2011). Nutrient analysis was conducted on samples without gas exchange measurements ($n = 3$) and on replicate samples after gas exchange measurements in order to analyze potential effects of the applied "wetting–drying" cycle. Nitrate (NO_3^-), nitrite (NO_2^-) and ammonium (NH_4^+) were analyzed via flow injection analysis with photometric detection (FIAstar 5000, Foss, Denmark). Prior to that, the samples comprised of soil and its biocrust cover were gently ground and an aliquot of 7 g was dissolved in 28 mL of 0.0125 M $CaCl_2$. After shaking

Table 1. Overview of the samples, distribution of replicates of soil–biocrust type and the different analyses.

Type	Only nutrient analysis	Flux measurements, followed by nutrient and chlorophyll analysis	Sum
Bare soil	3	3	6
Dark BSC	3	5	8
Light BSC	3	4	10
Light BSC + cyanolichen	3		
Chlorolichen BSC I	3	3	12
Chlorolichen BSC II		6	
Moss BSC	3	4	7
Sum	18	25	43

for 1 h the mixture was filtered on a N-free filter. The detection limits were 0.014, 0.046 and 0.047 mg kg^{-1} for NO_2^--N, NO_3^--N and NH_4^+-N, respectively.

Chlorophyll analysis, as an indicator of biomass of photoautotrophic organisms, was performed according to the dimethyl sulfoxide (DMSO) method (Ronen and Galun, 1984). Ground samples were extracted twice with $CaCO_3$-saturated DMSO (20, 10 mL) at 65 °C for 90 min. Both extracts were combined and centrifuged (3000 G) at 15 °C for 10 min. The light absorption at 648, 665 and 700 nm was detected with a spectral photometer (Lambda 25 UV/VIS Spectrometer, PerkinElmer, Rodgau). The amount of chlorophyll *a* (Chl_a) was calculated according to Arnon et al. (1974). Chlorophyll *a*+*b* (Chl_{a+b}) content was calculated according to O. L. Lange, W. Bilger, and H. Pfanz (personal communication with B. Weber, 1995; Weber et al., 2013):

$$\mathrm{Chl}_{a+b}\left[\mu g\right] = (20.2 \cdot (E_{648} - E_{700}) + 8.02 \cdot (E_{665} - E_{700})) \cdot a \quad (1)$$

$$\mathrm{Chl}_{a}\left[\mu g\right] = (12.19 \cdot (E_{665} - E_{700})) \cdot a, \quad (2)$$

where Chl_{a+b}[µg], Chl_a[µg] is the chlorophyll content of the sample; E_{648}, E_{665}, and E_{700} are light absorption at the given wavelength; and a is the amount of DMSO used (in milliliters).

The pH was determined for each surface cover type ($n = 3$–4) according to Weber et al. (2015, Supplement). Here, 1.5 g of the ground sample was mixed with 3.75 mL of pure water and shaken for 15 min. Then the slurry was centrifuged (3000 G, 5 min) to separate the solid phase from the liquid solution. The latter was used for pH determination by means of a pH electrode (InLab Expert Pro-ISM, Mettler Toledo).

2.4 Trace gas exchange measurements

The dynamic chamber method for analyzing NO and HONO emissions from soil samples was already introduced before (Oswald et al., 2013; Weber et al., 2015; Wu et al., 2014) and in general showed good agreement with flux measurements in the field (van Dijk et al., 2002; Rummel et al., 2002). Under the prevailing dry and hot conditions in Cyprus, macropores and cracks are likely to be present in the soil layer. It is assumed that during the sampling and sample treatment the number and sizes of soil cracks was not significantly increased so that the diffusivity of gases in the soil samples is comparable to the one in soil in the natural environment. Intact soil and biocrust samples (25–35 g in a plastic petri dish with 5.5 cm diameter and about 1 cm height) were wetted with 8–13 g of pure water (18.2 MΩ) up to full water holding capacity and placed into a dynamic Teflon film chamber (≈ 47 L) flushed with 8 L min^{-1} dry pure air (PAG 03, Eco Physics, Switzerland). Intact (biocrust) samples consist of a few millimeters of the biocrust and the underlying soil. Typical drying cycles lasted between 6 and 8 h. A Teflon-coated internal fan ensured complete mixing of the chamber headspace volume. During the experiments the chamber was kept at a constant temperature (25 °C, the mean daytime air temperature during CYPHEX) and in darkness to avoid photochemical reactions. At the chamber outlet the emitted gases HONO, NO and water vapor were quantified. HONO was analyzed with a commercial long path absorption photometer (LOPAP, Quma GmbH; Wuppertal, Germany) with a detection limit of ∼ 4 ppt and 10 % uncertainty (based on the uncertainties of liquid and gas flow, concentration of calibration standard, and regression of calibration). To avoid any transformation of HONO in the tubing, the sampling unit including the stripping coil from LOPAP was directly connected to the chamber. NO_x ($NO + NO_2$) was detected with a commercial chemiluminescence detector (42i-TL, Thermo Scientific; Waltham, USA) modified with a photolytic converter with a detection limit of ∼ 50 ppt (NO) and ∼ 200 ppt (NO_2). An infrared CO_2 and H_2O analyzer (Li-840A, Li-cor; Lincoln, USA) was used to log the drying and to calculate the soil water content (SWC) of the samples as follows:

$$\mathrm{SWC(WHC)} = \frac{m_{\mathrm{H_2O},\,t=n}}{m_{\mathrm{H_2O},0}} \cdot 100 \quad (3)$$

$$m_{\mathrm{H_2O},\,t=n} = m_{\mathrm{H_2O},\,t=n-1} - \frac{S_{\mathrm{Licor},\,t=n}}{\sum_{t=0}^{t=N} S_{\mathrm{Licor}}} \cdot m_{\mathrm{H_2O},0}, \quad (4)$$

with $t = 0$ denoting the measurement start (wetted sample inserted into chamber), $t = n$ any time between 0 and N, $t = N$ the time when the sample had dried out and measurement was stopped, S_{Licor} the absolute H_2O signal at a given time, $m_{H_2O,0}$ the mass of water added to the sample (water-holding capacity, WHC) and SWC the soil water content in % WHC.

2.5 Data analysis

Measured data of NO_2^-, NO_3^-, NH_4^+, Chl_{a+b}, Chl_a, NO and HONO optimum flux and NO and HONO integrated flux did not follow a normal distribution. Rather, log-transformed data were normally distributed (Shapiro–Wilk) and therefore used for statistical analysis (Pearson correlation, ANOVA including a Tukey test with a significance level of $p = 0.05$) executed with OriginPro (version 9.0; OriginLab Corporation, Northampton, Massachusetts, USA).

Precipitation data from the last 4 years (2013–2016), provided by the Department of Meteorology of Cyprus, indicating about 30 rain events per year (precipitation > 1 mm with following one or more dry days) were used to estimate annual emissions of total nitrogen in terms of HONO and NO.

3 Results and discussion

3.1 Meteorological conditions

About 1 month before sampling, three sensors measuring temperature and relative humidity were installed directly above the soil surface in the field to represent the microclimate of the ground surface. Reference air temperature, humidity and precipitation measurements at Paphos airport and Prodromos showed one rain event on 11–12 April, which is reflected by higher soil humidity (80–100 %) and lower temperatures on these days (see Fig. S2). As a consequence, the biological soil crusts were activated and went through one full wetting and drying cycle before sample collection. Temperature above the soil ranged from 10 °C at night to 50 °C during the day when solar radiation was most intense. Air temperature was similar at night but not as hot during the day, ranging between 20 and 30 °C. Humidity above the ground was low during the daytime (< 30 % rH) and increased during the night up to 80 %, while the atmospheric relative humidity (at Paphos airport) ranged between 47 and 73 % (without rain event). Thus, there were only little variations in humidity with height above the soil surface. Above the ground surface the relative humidity was somewhat lower during the day (mainly caused by higher temperatures) but somewhat higher at night, compared to respective weather station data. During and shortly after the main rain event humidity at ground level was higher (80 and 100 % rH) compared to ambient air humidity (70–85 % rH). Ambient air temperatures were somewhat lower during sample collection of this study as compared to the CYPHEX field campaign in 2014. During CYPHEX, nighttime temperatures (3 m a.g.l.) did not drop below 18 °C. Relative humidity (3 m a.g.l.) was mostly between 70 and 100 % with only two short periods with humidity between 20 and 60 % rH. Hence, we can assume that soil surface temperatures were higher and ground relative humidity in the same range during CYPHEX compared to sampling period.

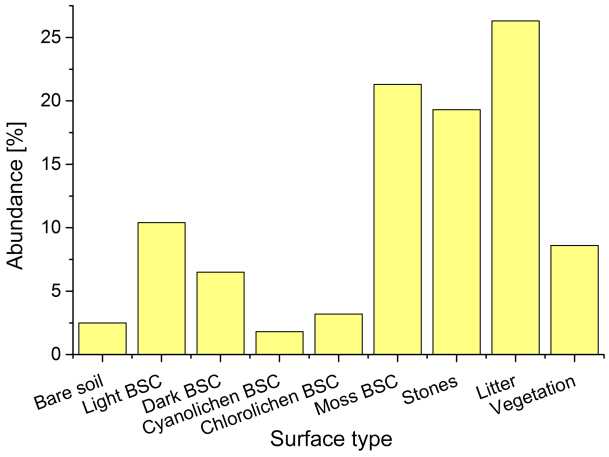

Figure 2. Distribution of different types of ground surfaces in the studied area. Information derived from 50 grids.

3.2 Cyprus soil and biocrust characteristics

The different biocrust types were distinguished in the field based on the dominating phototrophic compound but which provides no information about the microbial community below or about the magnitude of (de)nitrification processes. The microbial community could not be determined using nondestructive methods. Systematic mapping of surface covers revealed that moss-dominated biocrusts are the most frequent in the investigated Cyprus field site area (21.3 %), followed by light (10.4 %) and dark BSC (6.5 %), whereas chlorolichen- (3.2 %) and cyanolichen-dominated BSC (1.8 %) only played a minor role (Figs. 2 and S1). The soil surface was partially covered by litter (26.3 %), stones (19.5 %) and vascular vegetation (8.5 %), whereas open soil was rarely found (2.5 %). It was previously established that soil and biocrusts emit HONO and NO (Weber et al., 2015; Oswald et al., 2013), jointly accounting for 45.6 % of surface area in our studied region. To the best of our knowledge, no data on reactive nitrogen emissions from vascular vegetation and plant litter have been published yet.

Nutrient analysis revealed large variations in concentrations of nitrogen species ranging from 0 to 6.48, 0 to 0.57 and 0 to 22.2 mg (N) kg^{-1} of dry soil and crust mass for NO_3^-, NO_2^- and NH_4^+, respectively (Fig. 3a, Table S1 in the Supplement). In general, no significant change in reactive nitrogen contents was found before and after the trace gas exchange experiments, indicating no significant impact of one wetting–drying cycle on the nutrient content. Bare soil sam-

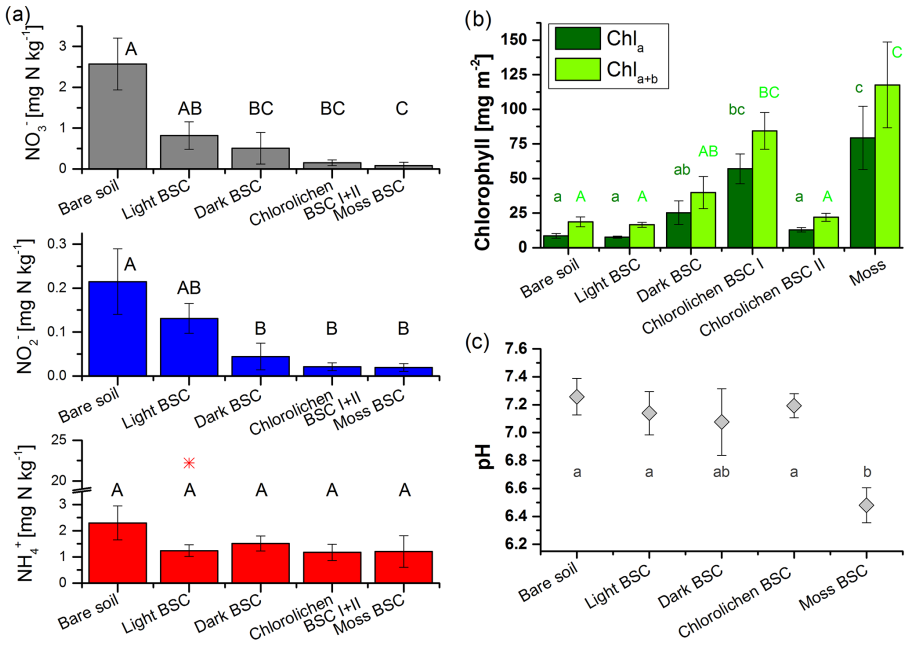

Figure 3. Nutrient and chlorophyll contents as well as pH values of bare soil and biocrust samples of different types. **(a)** Nitrate, nitrite and ammonium content of all replicates. The red star indicates an outlier; **(b)** chlorophyll a and chlorophyll $a+b$ contents of samples after flux measurements and **(c)** pH values of samples without and after flux measurements (bare soil and moss BSC: $n=4$; light, dark and chlorolichen BSC: $n=3$). For the number of replicates for a and b, see Table 1. In all three plots error bars indicate standard error of the mean and different letters indicate significant differences (of log-transformed data; $p=0.05$).

ples had significantly higher levels of NO_3^- and NO_2^- content compared to dark, chlorolichen and moss BSC. Among the latter three, no significant differences in nutrient levels were observed. Light BSC had NO_2^- contents similar to bare soil. The NH_4^+ content was very similar in all samples, except for one outlier in the group of light BSC with strongly elevated NH_4^+. Higher nitrate and ammonium levels in bare soil compared to crust-covered samples were also reported recently for a warm desert site in South Africa (Weber et al., 2015), indicative of nutrient consumption–integration by the biocrusts. Nitrite, however, was lower for bare soil samples compared to biocrust samples. While NO_3^- was slightly higher, NH_4^+ and NO_2^- contents (especially of bare soil samples) were lower in the South African arid ecosystem compared to Cyprus.

Chlorophyll was only determined in the samples used for flux measurements. Chl_a ranged from 4.1 (bare soil) to 144.2 mg m^{-2} (moss BSC) and Chl_{a+b} from 9.3 (bare soil) to 211.3 mg m^{-2} (moss BSC), respectively (Fig. 3b, Table S1). From bare soil, via light BSC and chlorolichen BSC II to dark BSC the chlorophyll content increased, but not significantly ($p>0.2$). Nevertheless, Chl_a and Chl_{a+b} contents of chlorolichen BSC I and moss BSC were significantly higher than those of bare soil, light BSC and chlorolichen BSC II ($p<0.05$, Fig. 3b). The range of chlorophyll contents is comparable to previous arid ecosystem studies (Weber et al., 2015).

The pH of soil and biocrusts ranged between slightly acidic (6.2) and slightly alkaline (7.6; Fig. 3c). The mean pH of 17 samples was 7.0, i.e., neutral. Only the pH of moss BSC samples was significantly lower than that of bare soil, light BSC and chlorolichen BSC samples ($p=0.05$). Soil and biocrust samples from South Africa were slightly more alkaline (7.1–8.2) with no significant difference among biocrust types (Weber et al., 2015).

3.3 NO and HONO flux measurements

All samples showed HONO and NO emissions during full wetting and drying cycles. The calculations of the emission or flux rates are shown in the Supplement. Maximum emission rates of HONO were observed at about 17–33 % WHC and of NO at 20–36 % with no significant differences among all soil cover types (Fig. 4). Emissions declined to zero at 0 % WHC and to very small rates for >70 %. Emission maxima strongly varied between soil cover types but also between samples of the same cover type (see Figs. 4 and 5 and Table S1). The highest emissions of both HONO-N and NO-N were detected for bare soil (175 ± 50.4 and 92.2 ± 20.0 ng m^{-2} s^{-1}; values indicate mean ± standard error), followed by light (48.6 ± 24.3 and 44.0 ± 22.4 ng m^{-2} s^{-1}) and dark BSC (27.1 ± 16.1 and 26.5 ± 15.9 ng m^{-2} s^{-1}). Both types of chlorolichen- and moss-dominated biocrusts showed very low emission rates

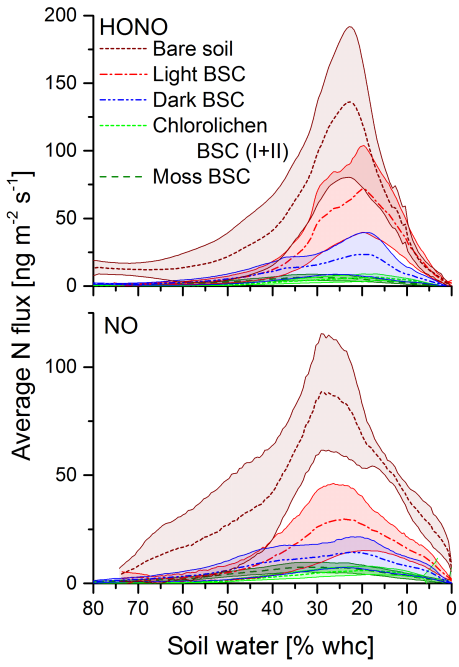

Figure 4. HONO and NO emission fluxes as a function of soil water content. Dotted lines are the mean fluxes. Shaded areas indicate the standard deviation.

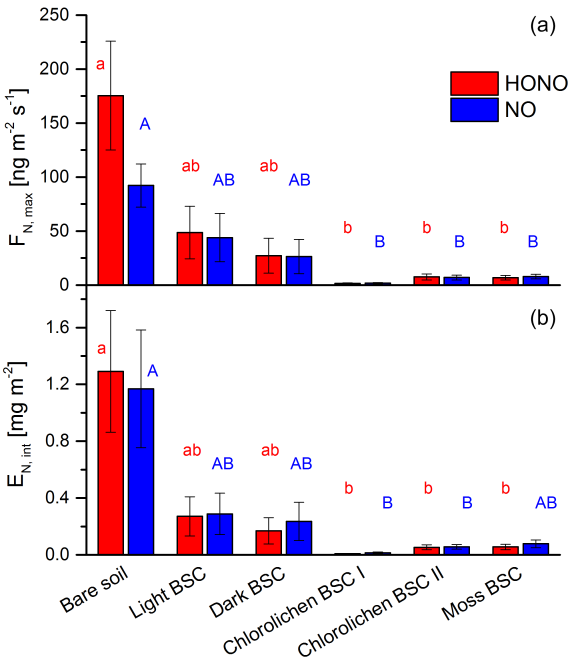

Figure 5. Emission of HONO and NO from bare soil and biocrusts. Panel **(a)** shows maximum HONO-N and NO-N fluxes (ng m^{-2} s^{-1}) at optimum water conditions. Panel **(b)** shows emissions integrated over a whole wetting–drying cycle (mg (N) m^{-2}); letters show significant difference ($p = 0.05$, of log-transformed data); error bars indicate standard error of the mean of replicates (bare soil $n = 3$; light BSC $n = 4$; dark BSC $n = 5$; chlorolichen BSC I $n = 3$; chlorolichen BSC II $n = 6$; moss BSC $n = 4$).

of reactive nitrogen (on average < 10 ng m^{-2} s^{-1}). Maximum HONO emissions were somewhat higher than maximum NO emissions, especially for bare soil. Integrating full wetting and drying cycles (6–8 h), 0.04–1.9 mg m^{-2} HONO-N and 0.06–1.6 mg m^{-2} NO-N was released (Fig. 5b). While the maximum fluxes of reactive nitrogen emission were higher for HONO than NO, especially from bare soil, the integrated emissions were similar or even larger for NO, which is released over a wider range of SWC.

In general, it is difficult to compare chamber flux measurements of different studies due to different experimental configurations, such as chamber dimension, flow rate, residence time, drying rate, etc. Here, we compared our results to studies that applied the same method (with the same or very similar conditions). The emission rates were consistent with the studies in which HONO-N or NO-N emissions from soil between 1 and 3000 ng m^{-2} s^{-1} were found (Su et al., 2011; Oswald et al., 2013; Mamtimin et al., 2016; Wu et al., 2014; Weber et al., 2015). Mamtimin et al. (2016) observed NO-N fluxes of 57.5, 18.9 and 4.1 ng m^{-2} s^{-1} at 25 °C for soil of grape and cotton fields and desert soil from an oasis in China, respectively. Oswald et al. (2013) found HONO-N and NO-N emissions between 2 and 280 ng m^{-2} s^{-1} (each) from different soil from all over the world covering a wide range of pH levels, nutrient content and organic matter. Biogenic NO emissions of 44 soil samples from arid and semi-arid regions were reviewed by Meixner and Yang (2006) with N fluxes ranging from 0 to 142 ng m^{-2} s^{-1}.

In contrast to the results of the present study, in which bare soil showed the highest emissions, Weber et al. (2015) found the lowest emissions from bare soil in samples from South Africa. In that study, dark cyanobacteria-dominated biocrusts revealed the highest emission rates (HONO-N and NO-N each up to 200 ng m^{-2} s^{-1}), followed by light cyanobacteria-dominated biocrusts (up to 120 ng m^{-2} s^{-1}), whereas in the present study, emissions of dark cyanobacteria-dominated biocrusts tended to be lower. No significant difference in HONO-N and NO-N emissions from light BSC between both sample origins were found. HONO-N and NO-N emissions of moss- and chlorolichen-dominated biocrusts were low in both studies (each < 60 ng m^{-2} s^{-1}) but still significantly higher for samples from South Africa than from Cyprus. In the present study HONO maximum emissions were higher than for NO (integrated emissions were comparable) while in the study of Weber et al. (2015) HONO maximum fluxes were somewhat lower than those of NO. The present results of nitrogen emissions correlated well with the nutrient contents (especially NO_2^- and NO_3^-, Fig. 6). Bare soil, in which the highest NO_3^- and NO_2^- levels were found, also showed the highest HONO and NO emissions. A good linear correlation was found between NO_2^- contents and emissions of both nitrogen gas-phase species for all samples ($R^2 = 0.84$

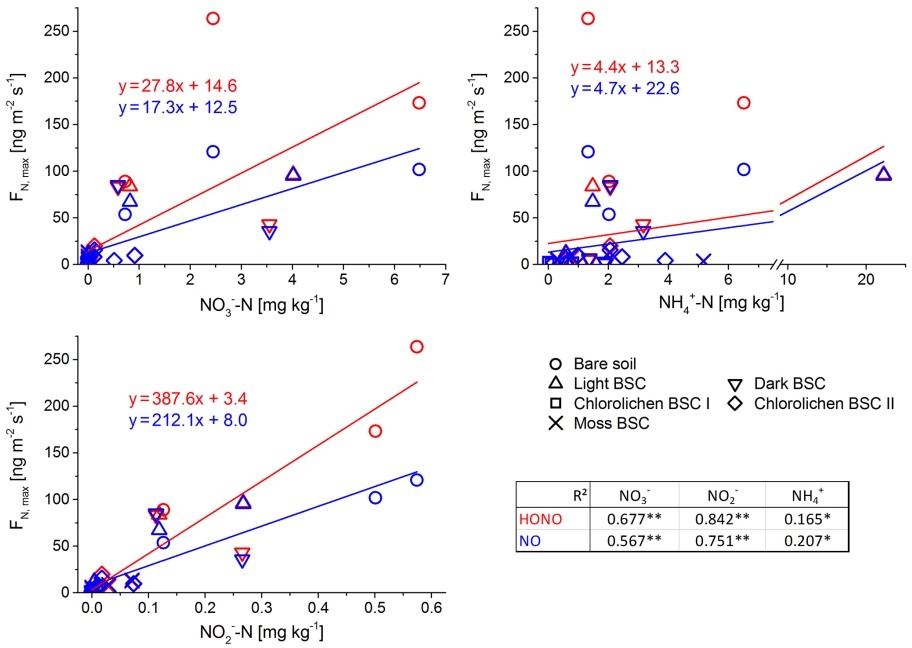

R^2	NO_3^-	NO_2^-	NH_4^+
HONO	0.677**	0.842**	0.165*
NO	0.567**	0.751**	0.207*

Figure 6. Correlation between maximum flux of HONO and NO and nutrient content of all Cyprus soil and biocrust samples with Pearson correlation factors (of log-transformed data; **: $p<0.001$; *: $p<0.05$).

for HONO and 0.85 for NO; $p<0.001$). The level of correlation between NO_3^- and HONO and NO was lower, but still significant ($R^2=0.68$ and 0.67, respectively; $p<0.001$). Low correlations were found between HONO or NO emissions and NH_4^+ contents ($R^2=0.165$ and 0.232; $p=0.05$). Thus, in the present study it seems that reactive nitrogen emissions predominantly depend on NO_2^- and NO_3^- contents and not on surface cover types, although biocrusts (especially with cyanobacteria and cyanolichens) are able to fix atmospheric nitrogen (Belnap, 2002; Elbert et al., 2012; Barger et al., 2013; Patova et al., 2016). The results of a two-factorial ANOVA showed that HONO or NO emissions were not significantly related to soil cover type but rather to nitrite content, i.e., its direct aqueous precursor. For nitrate, the two-factorial ANOVA indicated dependencies of both cover type and nutrient content. Long-range transport and instantaneous atmospheric deposition of NO_x NO_3^-, NO_2^- and NH_4^+ can be excluded to be a dominant source of HONO and NO precursors in local soil, as the observed concentrations in Cyprus ambient air were very low (Meusel et al., 2016; Kleanthous et al., 2014). A dominant contribution from microbial activity to the nutrient content is anticipated, although long-term atmospheric accumulation of nutrients in the soil prior to the field campaign cannot be excluded. While biocrusts increase nutrient availability via N fixation, it is their possible associations with ammonia-oxidizing microbes (bacterial and archaea) that finally convert the fixed nitrogen to nitrite and nitrate. Determination of the microbial community below the biocrust or in bare soil was not carried out as it was outside the scope of this study. Nitrification and other nitrogen cycling processes are not restricted to biocrusts and can also occur in non-crusted soils. The relevance of these processes is expected to depend on substrate richness (i.e., amount of ammonium available for nitrifiers). Our results differ from those obtained by Weber et al. (2015) on South African samples, as their HONO and NO emissions were not correlated with bulk concentrations of ammonium, nitrite and nitrate. In their study nitrite content was lowest for bare soil compared to other biocrust types. Ammonium and nitrite levels were also lower than in the present study. Therefore, Weber et al. (2015) indicated that biocrusts can enhance the N cycle and emission of reactive nitrogen.

Since most of the samples were slightly alkaline and only moss samples were slightly acidic, no effect of pH could be observed. However, in general it is expected that with higher nutrient and lower pH values HONO emission is increased by simple partitioning processes (Su et al., 2011). The simulated equilibrium concentration at soil surface [HONO]* (Eqs. S1 and S4 in Su et al., 2011) is much lower than the measured one (see Fig. S3). This deviation is probably based on the nonideal behavior of the soil samples (adsorption, Kelvin and solute interaction effects on gas–liquid partitioning). However, this method does not allow argumentation on physical or biological processes.

3.4 Comparison of soil emissions and observed missing source

To quantify the flux rate of HONO emissions from soil to the local atmosphere and to compare it to the unaccounted-

for source found in Cyprus in 2014 (Meusel et al., 2016), we applied a standard formalism describing the atmosphere–soil exchange of trace gases as a function of the difference between the atmospheric concentration and the equilibrium concentration at the soil solution surface [HONO]* (Su et al., 2011):

$$F^* = v_t([HONO]^* - [HONO]), \quad (5)$$

where [HONO] is the ambient HONO concentration measured on Cyprus (mean daytime average 60 ppt) and [HONO]* is the equilibrium concentration at soil surface. [HONO]* can be determined from measurements in a static chamber. In a dynamic chamber system, there is a concentration gradient of HONO between the headspace (where HONO was measured) and the soil surface. Here we used the measurements of water vapor to correct for the soil surface concentration and equilibrium concentration of HONO by assuming a similar gradient for the two species. A correction coefficient of 3.8 was determined, which is the ratio of the equilibrium relative humidity of 100 % over wet soil surface to the initial headspace relative humidity of 25–30 % after inserting the wet sample into the chamber. The transfer velocity, v_t, depends primarily on meteorological and soil conditions and is typically on the order of $\sim 1\,\mathrm{cm\,s^{-1}}$. The flux rate of NO was calculated accordingly with mean daytime NO concentrations of 38 ppt. The calculated flux F* was about (67 ± 3) % of the flux measured in the chamber.

The distribution of nine different surface cover types was mapped (Fig. 2), including stones, vascular vegetation and litter not being attributed to emit significant amounts of HONO and NO to the atmosphere. The residual HONO-emitting surface covers comprised 45.6 % of total surface in the investigated area. Combining the information on soil–biocrust population and the calculated flux F*, a site-specific community emission F_{comm} of HONO and NO can be estimated via following equation (Eq. 6).

$$F_{comm,\,max} = \sum_{i}^{type} F^*_{max,i} \cdot p_i/100$$
$$\text{or } F_{comm,\,int} = \sum_{i}^{type} F^*_{int,i} \cdot p_i/100, \quad (6)$$

where F_{comm} denotes the estimated community flux, $F^*_{max,i\ or\ int,i}$ the maximum or integrated emission rates of each individual surface cover type i ($\mathrm{ng\,N\,m^{-2}\,s^{-1}}$ or $\mathrm{\mu g\,N\,m^{-2}}$) and p_i the fraction of population type i (%).

Under optimum soil water conditions (20–30 % WHC) and constant temperatures of about 25 °C, between 2.2 and $18.8\,\mathrm{ng\,m^{-2}\,s^{-1}}$ of total HONO-N and between 1.6 and $16.2\,\mathrm{ng\,m^{-2}\,s^{-1}}$ of total NO-N are emitted from the different crust–soil population combinations derived from the vegetation cover assessment. In the lower range of total emissions the contribution from bare soil dominates with up to 69 % (HONO) and 55 % (NO), followed by moss BSC (HONO: 23 %; NO: 32 %). At high levels of total emissions, the contribution from light BSC dominates (HONO: 43 %; NO: 49 %), decreasing the contribution of bare soil down to about 25 % (HONO) and 13 % (NO). Emissions from dark BSC contribute about 20 or 24 % to the total HONO or NO flux while the contribution from moss BSC decreases to 10 or 12 %. Emissions from chlorolichen BSC do not play a significant role (< 2.4 %) in general (see Fig. 7).

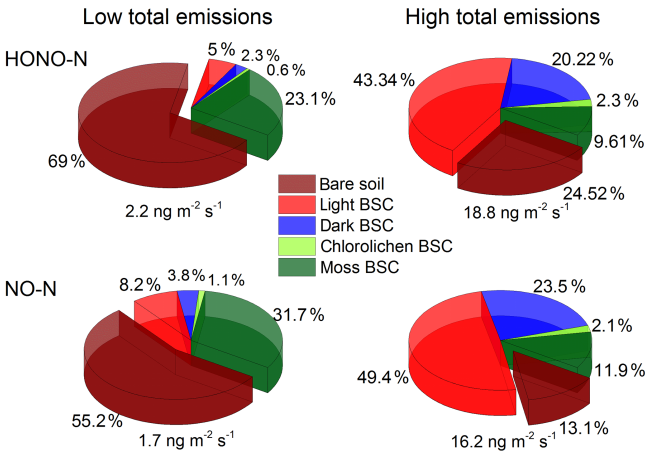

Figure 7. Contributions of different ground surfaces to the total F*.

After heavy rainfalls moistening the soil to full WHC, 11–113 $\mathrm{\mu g\,m^{-2}}$ of HONO-N and 10–131 $\mathrm{\mu g\,m^{-2}}$ of NO-N can be calculated for one complete wetting–drying period. Assuming 30 rain events per year (based on the statistic of 4 years of precipitation data), a wetting–drying cycle time of 7 days, and constant emissions in between them (at 10 % WHC), up to $160\,\mathrm{mg\,m^{-2}\,yr^{-1}}$ of nitrogen can be emitted directly by the sum of HONO-N and NO-N from Cyprus natural ground surfaces, i.e., excluding heterogeneous conversion of NO_2 on ground surface.

The release of HONO from the ground surface to the atmosphere can be related to the atmospheric HONO production rate via Eq. (7) (adapted from Su et al., 2011) and then compared to the missing source.

$$S_{ground} = \frac{F_{comm,\,max}(T,\,swc)}{BLH} \cdot a, \quad (7)$$

with S_{ground} as the HONO or NO emitted from ground surface; BLH the boundary layer height (mixed layer height) and a the factor to convert nanograms of nitrogen into the number of molecules ($10^{-9} \cdot 6.022 \times 10^{23}/14$).

During the CYPHEX campaign in summer 2014 a mean boundary layer height of 300 m a.g.l. was observed by means of a ceilometer. Due to missing precipitation during CYPHEX, but high relative humidity prevailing (CYPHEX 2014: 75–100 %), a mean SWC of 10 % WHC (at 25 °C) can be estimated (Likos, 2008; Leelamanie, 2010), reducing the HONO source strength to 35 % of the emission

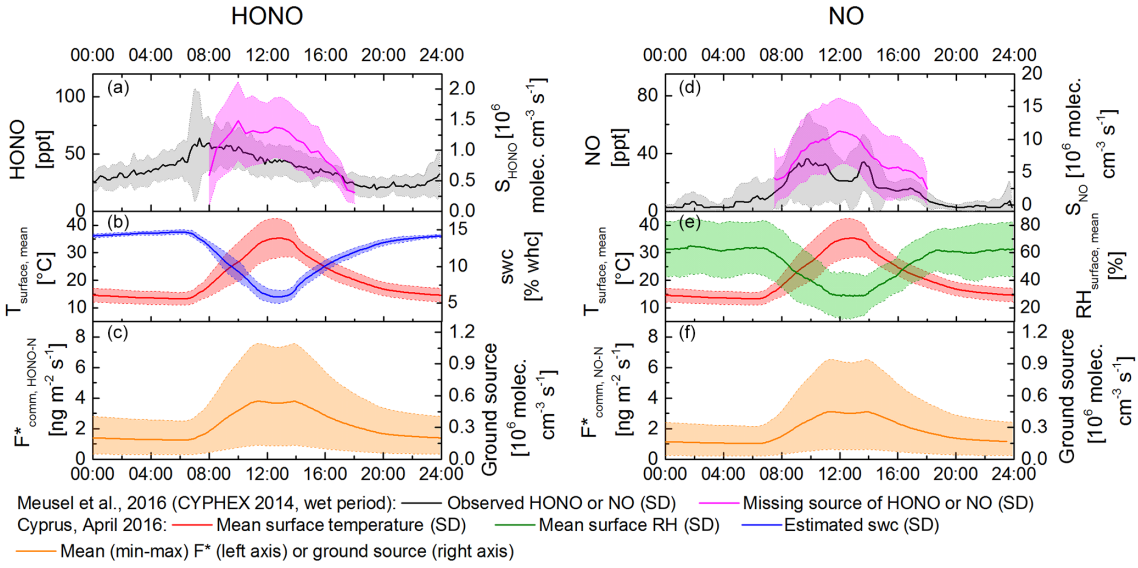

Figure 8. Diel pattern for HONO and NO emissions in comparison with the observed HONO concentrations and missing source during the CYPHEX 2014 campaign. Panels **(a, d)** show observed concentration of HONO and NO in black; missing source shown in pink. Panels **(b, e)** show mean surface temperature and mean surface humidity measured in April 2016 in Cyprus and estimated soil water content in red, green and blue, respectively. Panels **(c, f)** show the calculated mean F* (mean temperature) with the shaded area indicating the lower and upper limits.

maximum at optimum SWC. Integrating the lowermost versus the uppermost observed HONO emissions per soil–crust type, the emissions at 25 °C and a SWC of 10 % WHC would span a wide range between 1.1×10^5 and 9.6×10^5 molecules cm^{-3} s^{-1}, covering 9 to 73 % of the missing mean source of 1.3×10^6 molecules cm^{-3} s^{-1} observed in the field (Meusel et al., 2016). However, temperatures in the field have strong diel cycles, and a temperature increase from 25 to 50 °C has been shown to lead to 6–10 times higher emissions at constant SWC (Oswald et al., 2013; Mamtimin et al., 2016). On Cyprus the observed soil surface temperatures changed from 10 °C at night up to 45 °C during the daytime (Fig. 8, red line, or Fig. S2). In the natural habitat the micrometeorological parameters change in concert, i.e., with increasing temperature the SWC decreases, influencing the flux-enhancing effect of temperature. Based on the assumption of a linear change of SWC with temperature, a diel course of the SWC between 6 and 14 % of WHC is simulated (Fig. 8, blue line), lowering the emission flux (22–49 % of optimum). Applying the described SWC dependence and the temperature dependence on flux rates as reported by Oswald et al. (2013), high daytime temperatures increase the simulated diel course of HONO-N flux up to a daytime maximum of 7.4 ng m^{-2} s^{-1} (Fig. 8, lower panel), but with a notable dip at high noon due to the opposing effect of decreasing SWC at higher temperatures. The NO-N emissions show a similar pattern, with a slightly lower flux range (up to 6.4 ng m^{-2} s^{-1}). Converted into production rates (Eq. 7), the ground-based soil and biocrust emissions at noon would be up to 1.1×10^6 molecules cm^{-3} s^{-1} HONO-N and 0.9×10^6 molecules cm^{-3} s^{-1} NO-N covering up to 85 and 8.5 % of the missing HONO and NO source found during CYPHEX 2014 (Meusel et al., 2016). Note that during CYPHEX there were two periods with lower relative humidity, in which even a NO sink was detected. In some mornings of the campaign dew formation was expected, causing an increase in soil humidity. Combined with rising temperatures after sunrise, these optimized meteorological conditions may have led to enhanced soil emissions and would confer a reasonable explanation for the strong HONO morning peaks observed during the campaign.

Field observations (VandenBoer et al., 2013; Zhang et al., 2009; Tsai et al. 2017) as well as model results (Wong et al., 2013) showed that HONO concentrations typically decrease exponentially from the surface upwards. Equation (7) does not include a chemistry–transport model nor accounts for the existence of a vertical profile of concentrations, which may bias the calculation on HONO source strength. However, the method for predicting the ground source using homogeneous mixed air columns is consistent with other recent studies (Stemmler et al., 2006; Tsai et al., 2017). Tsai et al. (2017) clearly showed the presence of an important ground source of daytime HONO at a rural basin in Utah during winter (no snow, low temperatures). They inferred that ground surface fluxes may account for 63 ± 32 % of the unidentified HONO daytime source throughout the day. HONO-N fluxes of up to 7.4 ng m^{-2} s^{-1} (Fig. 8c) determined in this study are comparable to HONO-N fluxes found in other regions,

e.g., 2.7 ng m^{-2} s^{-1} reported for the northern Michigan forest canopy (Zhang et al., 2009; Zhou et al., 2011), the average daytime HONO-N flux of 7.0 ng m^{-2} s^{-1} measured over an agricultural field in Bakersfield (Ren et al., 2011) and the average HONO-N flux of about 11.6 ng m^{-2} s^{-1} measured by Tsai et al. (2017). In contrast to the present study, the latter concluded that, under the prevailing high NO_x conditions, the respective HONO formation was related to solar radiation and NO_2 mixing ratios, such as photo-enhanced conversion of NO_2 or nitrate photolysis on the ground. This can be ruled out in this study, as pure air (no NO_2) was used to purge the chambers and no light was applied. While in Cyprus the observed soil emissions can explain high amounts of atmospheric HONO, other studies excluded soil emission as a dominant source (Oswald et al., 2015; Laufs et al., 2017). Oswald et al. (2015) studied soil samples from a boreal forest in Finland and observed HONO emissions below the detection limit. However, those samples had very low nutrient contents and were highly acidic (pH $\approx$ 3), for which microbial activity is supposed to be low (Fierer and Jackson, 2006; Persson and Wirén, 1995; Ste-Marie and Pare, 1999; Šimek and Cooper, 2002). Similarly, Laufs et al. (2017) did not find correlations between HONO fluxes and temperature or humidity measured in the field and concluded that HONO sources other than biological soil emissions must have dominated. In contrast to the SWC in Cyprus, the water contents at the field site studied by Laufs et al. (2016) were higher than the optimum SWC presented by Oswald et al. (2013).

4 Conclusions

HONO and NO emission rates from soil and biological soil crusts were derived by means of lab-based enclosure trace gas exchange measurements, and they revealed quite similar ranges of reactive nitrogen source strengths. Emissions of both compounds strongly correlated with NO_2^- and NO_3^- content of the samples. Emissions from bare soil were highest, but bare soil surface spots were rarely found at the investigated CYPHEX field study site. The estimated total ground surface HONO flux in the natural habitat was consistent with the previously unaccounted-for source estimated for Cyprus, i.e., the unaccounted-for HONO source can essentially be explained by emissions from soil and biocrusts. For NO, the measured and simulated fluxes cannot account for the unaccounted-for NO source (during the humid periods of the CYPHEX campaign 2014), indicating that emissions from soil were not the only missing source of NO.

Data availability. For detailed information on data please contact Hang Su (h.su@mpic.de).

Supplement. The supplement related to this article is available online at: https://doi.org/10.5194/acp-18-799-2018-supplement.

Competing interests. The authors declare that they have no conflict of interest.

Acknowledgements. The accompanied campaign in Cyprus 2016 was supported by the INUIT-BCCHUS-ACTRIS project.

The article processing charges for this open-access publication were covered by the Max Planck Society.

Edited by: James Roberts
Reviewed by: three anonymous referees

References

Abed, R. M. M., Lam, P., de Beer, D., and Stief, P.: High rates of denitrification and nitrous oxide emission in arid biological soil crusts from the Sultanate of Oman, Isme Journal, 7, 1862–1875, https://doi.org/10.1038/ismej.2013.55, 2013.

Alicke, B., Platt, U., and Stutz, J.: Impact of nitrous acid photolysis on the total hydroxyl radical budget during the Limitation of Oxidant Production/Pianura Padana Produzione di Ozono study in Milan, J. Geophys. Res.-Atmos., 107, 8196, https://doi.org/10.1029/2000jd000075, 2002.

Ammann, M., Kalberer, M., Jost, D. T., Tobler, L., Rossler, E., Piguet, D., Gaggeler, H. W., and Baltensperger, U.: Heterogeneous production of nitrous acid on soot in polluted air masses, Nature, 395, 157–160, https://doi.org/10.1038/25965, 1998.

Arens, F., Gutzwiller, L., Baltensperger, U., Gaggeler, H. W., and Ammann, M.: Heterogeneous reaction of NO_2 on diesel soot particles, Environ. Sci. Technol., 35, 2191–2199, https://doi.org/10.1021/es000207s, 2001.

Aubin, D. G. and Abbatt, J. P. D.: Interaction of NO_2 with hydrocarbon soot: Focus on HONO yield, surface modification, and mechanism, J. Phys. Chem. A, 111, 6263–6273, https://doi.org/10.1021/jp068884h, 2007.

Baergen, A. M. and Donaldson, D. J.: Photochemical renoxification of nitric acid on real urban grime, Environ. Sci. Technol., 47, 815–820, https://doi.org/10.1021/es3037862, 2013.

Barger, N. N., Castle, S. C., and Dean, G. N.: Denitrification from nitrogen-fixing biologically crusted soils in a cool desert environment, southeast Utah, USA, Ecological Processes, 2, 16, https://doi.org/10.1186/2192-1709-2-16, 2013.

Barger, N. N., Weber, B., Garcia-Pichel, F., Zaady, E., and Belnap, J.: Patterns and controls on nitrogen cycling of biological soil crusts, in: Biological soil crusts: An organizing principle in drylands, edited by: Weber, B., Büdel, B., and Belnap, J., Ecological Studies 226, Springer International Publishing Switzerland, 257–285, 2016.

Bejan, I., Abd El Aal, Y., Barnes, I., Benter, T., Bohn, B., Wiesen, P., and Kleffmann, J.: The photolysis of ortho-nitrophenols: a new gas phase source of HONO, Phys. Chem. Chem. Phys., 8, 2028–2035, https://doi.org/10.1039/b516590c, 2006.

Belnap, J.: Nitrogen fixation in biological soil crusts from southeast Utah, USA, Biol. Fert. Soils, 35, 128–135, https://doi.org/10.1007/s00374-002-0452-x, 2002.

Belnap, J., Weber, B., Büdel, B. (Eds.): Biological soil crusts as an organizing principle in drylands, in: Biological soil crusts: An organizing principle in drylands, Ecological Studies 226, Springer International Publishing Switzerland, 3–13, 2016.

Brankatschk, R., Fischer, T., Veste, M., and Zeyer, J.: Succession of N cycling processes in biological soil crusts on a Central European inland dune, FEMS Microbiol. Ecol., 83, 149–160, 2013.

Bröske, R., Kleffmann, J., and Wiesen, P.: Heterogeneous conversion of NO_2 on secondary organic aerosol surfaces: A possible source of nitrous acid (HONO) in the atmosphere?, Atmos. Chem. Phys., 3, 469–474, https://doi.org/10.5194/acp-3-469-2003, 2003.

Büdel, B., Darienko, T., Deutschewitz, K., Dojani, S., Friedl, T., Mohr, K., Salisch, M., Reisser, W., and Weber, B.: Southern African biological soil crusts are ubiquitous and highly diverse in drylands, being restricted by rainfall frequency, FEMS Microbiol. Ecol., 57, 229–247, 2009.

Cleveland, C. C., Townsend, A. R., Schimel, D. S., Fisher, H., Howarth, R. W., Hedin, L. O., Perakis, S. S., Latty, E. F., Von Fischer, J. C., Elseroad, A., and Wasson, M. F.: Global patterns of terrestrial biological nitrogen (N_2) fixation in natural ecosystems, Global Biogeochem. Cy., 13, 623–645, https://doi.org/10.1029/1999gb900014, 1999.

Czader, B. H., Rappenglück, B., Percell, P., Byun, D. W., Ngan, F., and Kim, S.: Modeling nitrous acid and its impact on ozone and hydroxyl radical during the Texas Air Quality Study 2006, Atmos. Chem. Phys., 12, 6939–6951, https://doi.org/10.5194/acp-12-6939-2012, 2012.

Elbert, W., Weber, B., Burrows, S., Steinkamp, J., Budel, B., Andreae, M. O., and Pöschl, U.: Contribution of cryptogamic covers to the global cycles of carbon and nitrogen, Nat. Geosci., 5, 459–462, 2012.

Fierer, N. and Jackson, R. B.: The diversity and biogeography of soil bacterial communities, P. Natl. Acad. Sci. USA, 103, 626–631, https://doi.org/10.1073/pnas.0507535103, 2006.

George, C., Strekowski, R. S., Kleffmann, J., Stemmler, K., and Ammann, M.: Photoenhanced uptake of gaseous NO_2 on solid-organic compounds: a photochemical source of HONO?, Faraday Discuss., 130, 195–210, https://doi.org/10.1039/b417888m, 2005.

Han, C., Yang, W. J., Wu, Q. Q., Yang, H., and Xue, X. X.: Heterogeneous photochemical conversion of NO_2 to HONO on the humic acid surface under simulated sunlight, Environ. Sci. Technol., 50, 5017–5023, https://doi.org/10.1021/acs.est.5b05101, 2016.

Harrison, R. M. and Kitto, A. M. N.: Evidence for a surface source of atmospheric nitrous acid, Atmos. Environ., 28, 1089–1094, https://doi.org/10.1016/1352-2310(94)90286-0, 1994.

Herridge, D. F., Peoples, M. B., and Boddey, R. M.: Global inputs of biological nitrogen fixation in agricultural systems, Plant Soil, 311, 1–18, https://doi.org/10.1007/s11104-008-9668-3, 2008.

Johnson, S. L., Budinoff, C. R., Belnap, J., and Garcia-Pichel, F.: Relevance of ammonium oxidation within biological soil crust communities, Environ. Microbiol., 7, 1–12, https://doi.org/10.1111/j.1462-2920.2004.00649.x, 2005.

Kalberer, M., Ammann, M., Arens, F., Gaggeler, H. W., and Baltensperger, U.: Heterogeneous formation of nitrous acid (HONO) on soot aerosol particles, J. Geophys. Res.-Atmos., 104, 13825–13832, https://doi.org/10.1029/1999jd900141, 1999.

Kebede, M. A., Scharko, N. K., Appelt, L. E., and Raff, J. D.: Formation of nitrous acid during ammonia photooxidation on TiO_2 under atmospherically relevant conditions, J. Phys. Chem. Lett., 4, 2618–2623, https://doi.org/10.1021/jz401250k, 2013.

Kinugawa, T., Enami, S., Yabushita, A., Kawasaki, M., Hoffmann, M. R., and Colussi, A. J.: Conversion of gaseous nitrogen dioxide to nitrate and nitrite on aqueous surfactants, Phys. Chem. Chem. Phys., 13, 5144–5149, https://doi.org/10.1039/C0CP01497D, 2011.

Kleanthous, S., Vrekoussis, M., Mihalopoulos, N., Kalabokas, P., and Lelieveld, J.: On the temporal and spatial variation of ozone in Cyprus, Sci. Total Environ., 476–477, 677–687, https://doi.org/10.1016/j.scitotenv.2013.12.101, 2014.

Kleffmann, J. and Wiesen, P.: Heterogeneous conversion of NO_2 and NO on HNO_3 treated soot surfaces: atmospheric implications, Atmos. Chem. Phys., 5, 77–83, https://doi.org/10.5194/acp-5-77-2005, 2005.

Kleffmann, J., Becker, K. H., Lackhoff, M., and Wiesen, P.: Heterogeneous conversion of NO_2 on carbonaceous surfaces, Phys. Chem. Chem. Phys., 1, 5443–5450, https://doi.org/10.1039/A905545B, 1999.

Kleffmann, J., Kurtenbach, R., Lorzer, J., Wiesen, P., Kalthoff, N., Vogel, B., and Vogel, H.: Measured and simulated vertical profiles of nitrous acid – Part I: Field measurements, Atmos. Environ., 37, 2949–2955, https://doi.org/10.1016/s1352-2310(03)00242-5, 2003.

Kleffmann, J., Gavriloaiei, T., Hofzumahaus, A., Holland, F., Koppmann, R., Rupp, L., Schlosser, E., Siese, M., and Wahner, A.: Daytime formation of nitrous acid: A major source of OH radicals in a forest, Geophys. Res. Lett., 32, L05818, https://doi.org/10.1029/2005gl022524, 2005.

Langridge, J. M., Gustafsson, R. J., Griffiths, P. T., Cox, R. A., Lambert, R. M., and Jones, R. L.: Solar driven nitrous acid formation on building material surfaces containing titanium dioxide: A concern for air quality in urban areas?, Atmos. Environ., 43, 5128–5131, https://doi.org/10.1016/j.atmosenv.2009.06.046, 2009.

Laufs, S., Cazaunau, M., Stella, P., Kurtenbach, R., Cellier, P., Mellouki, A., Loubet, B., and Kleffmann, J.: Diurnal fluxes of HONO above a crop rotation, Atmos. Chem. Phys., 17, 6907–6923, https://doi.org/10.5194/acp-17-6907-2017, 2017.

Leelamanie, D. A. L.: Changes in Soil Water Content with Ambient Relative Humidity in Relation to the Organic Matter and Clay, Tropical Agricultural Research and Extension, 13, 6–10, https://doi.org/10.4038/tare.v13i1.3130, 2010.

Lelièvre, S., Bedjanian, Y., Laverdet, G., and Le Bras, G.: Heterogeneous reaction of NO_2 with hydrocarbon flame soot, J. Phys. Chem. A, 108, 10807–10817, https://doi.org/10.1021/jp0469970, 2004.

Li, X., Rohrer, F., Hofzumahaus, A., Brauers, T., Häseler, R., Bohn, B., Broch, S., Fuchs, H., Gomm, S., Holland, F., Jäger, J., Kaiser, J., Keutsch, F. N., Lohse, I., Lu, K., Tillmann, R., Wegener, R., Wolfe, G. M., Mentel, T. F., Kiendler-Scharr, A., and Wahner, A.: Missing gas-phase source of HONO inferred from Zeppelin measurements in the troposphere, Science, 344, 292–296, https://doi.org/10.1126/science.1248999, 2014.

Likos, W. J.: Vapor adsorption index for expansive soil classification, J. Geotech. Geoenviron., 134, 1005–1009, https://doi.org/10.1061/(asce)1090-0241(2008)134:7(1005), 2008.

Liu, Y., Han, C., Ma, J., Bao, X., and He, H.: Influence of relative humidity on heterogeneous kinetics of NO_2 on kaolin and hematite, Phys. Chem. Chem. Phys., 17, 19424–19431, https://doi.org/10.1039/c5cp02223a, 2015.

Mamtimin, B., Meixner, F. X., Behrendt, T., Badawy, M., and Wagner, T.: The contribution of soil biogenic NO and HONO emissions from a managed hyperarid ecosystem to the regional NO_x emissions during growing season, Atmos. Chem. Phys., 16, 10175–10194, https://doi.org/10.5194/acp-16-10175-2016, 2016.

Meixner, F. X. and Yang, W. X.: Biogenic emissions of nitric oxide and nitrous oxide from arid and semi-arid land, in: Dryland Ecohydrology, edited by: D'Odorico, P. and Porporato, A., Springer Netherlands, Dordrecht, 233–255, 2006.

Meusel, H., Kuhn, U., Reiffs, A., Mallik, C., Harder, H., Martinez, M., Schuladen, J., Bohn, B., Parchatka, U., Crowley, J. N., Fischer, H., Tomsche, L., Novelli, A., Hoffmann, T., Janssen, R. H. H., Hartogensis, O., Pikridas, M., Vrekoussis, M., Bourtsoukidis, E., Weber, B., Lelieveld, J., Williams, J., Pöschl, U., Cheng, Y., and Su, H.: Daytime formation of nitrous acid at a coastal remote site in Cyprus indicating a common ground source of atmospheric HONO and NO, Atmos. Chem. Phys., 16, 14475–14493, https://doi.org/10.5194/acp-16-14475-2016, 2016.

Meusel, H., Elshorbany, Y., Kuhn, U., Bartels-Rausch, T., Reinmuth-Selzle, K., Kampf, C. J., Li, G., Wang, X., Lelieveld, J., Pöschl, U., Hoffmann, T., Su, H., Ammann, M., and Cheng, Y.: Light-induced protein nitration and degradation with HONO emission, Atmos. Chem. Phys., 17, 11819–11833, https://doi.org/10.5194/acp-17-11819-2017, 2017.

Michoud, V., Colomb, A., Borbon, A., Miet, K., Beekmann, M., Camredon, M., Aumont, B., Perrier, S., Zapf, P., Siour, G., Ait-Helal, W., Afif, C., Kukui, A., Furger, M., Dupont, J. C., Haeffelin, M., and Doussin, J. F.: Study of the unknown HONO daytime source at a European suburban site during the MEGAPOLI summer and winter field campaigns, Atmos. Chem. Phys., 14, 2805–2822, https://doi.org/10.5194/acp-14-2805-2014, 2014.

Monge, M. E., D'Anna, B., Mazri, L., Giroir-Fendler, A., Ammann, M., Donaldson, D. J., and George, C.: Light changes the atmospheric reactivity of soot, P. Natl. Acad. Sci. USA, 107, 6605–6609, https://doi.org/10.1073/pnas.0908341107, 2010.

Ndour, M., D'Anna, B., George, C., Ka, O., Balkanski, Y., Kleffmann, J., Stemmler, K., and Ammann, M.: Photoenhanced uptake of NO_2 on mineral dust: Laboratory experiments and model simulations, Geophys. Res. Lett., 35, L05812, https://doi.org/10.1029/2007gl032006, 2008.

Neuman, J. A., Trainer, M., Brown, S. S., Min, K. E., Nowak, J. B., Parrish, D. D., Peischl, J., Pollack, I. B., Roberts, J. M., Ryerson, T. B., and Veres, P. R.: HONO emission and production determined from airborne measurements over the Southeast U.S, J. Geophys. Res.-Atmos., 121, 9237–9250, https://doi.org/10.1002/2016JD025197, 2016.

Oswald, R., Behrendt, T., Ermel, M., Wu, D., Su, H., Cheng, Y., Breuninger, C., Moravek, A., Mougin, E., Delon, C., Loubet, B., Pommerening-Roeser, A., Soergel, M., Poeschl, U., Hoffmann, T., Andreae, M. O., Meixner, F. X., and Trebs, I.: HONO emissions from soil bacteria as a major source of atmospheric reactive nitrogen, Science, 341, 1233–1235, https://doi.org/10.1126/science.1242266, 2013.

Oswald, R., Ermel, M., Hens, K., Novelli, A., Ouwersloot, H. G., Paasonen, P., Petäjä, T., Sipilä, M., Keronen, P., Bäck, J., Königstedt, R., Hosaynali Beygi, Z., Fischer, H., Bohn, B., Kubistin, D., Harder, H., Martinez, M., Williams, J., Hoffmann, T., Trebs, I., and Sörgel, M.: A comparison of HONO budgets for two measurement heights at a field station within the boreal forest in Finland, Atmos. Chem. Phys., 15, 799–813, https://doi.org/10.5194/acp-15-799-2015, 2015.

Patova, E., Sivkov, M., and Patova, A.: Nitrogen fixation activity in biological soil crusts dominated by cyanobacteria in the Subpolar Urals (European North-East Russia), FEMS Microbiol. Ecol., 92, fiw131, https://doi.org/10.1093/femsec/fiw131, 2016.

Persson, T. and Wirén, A.: Nitrogen mineralization and potential nitrification at different depths in acid forest soils, Plant Soil, 168, 55–65, https://doi.org/10.1007/bf00029313, 1995.

Pilegaard, K.: Processes regulating nitric oxide emissions from soils, Philos. T. R. Soc. B: Biological Sciences, 368, 20130126, https://doi.org/10.1098/rstb.2013.0126, 2013.

Ramazan, K. A., Syomin, D., and Finlayson-Pitts, B. J.: The photochemical production of HONO during the heterogeneous hydrolysis of NO_2, Phys. Chem. Chem. Phys., 6, 3836–3843, https://doi.org/10.1039/b402195a, 2004.

Ren, X. R., Harder, H., Martinez, M., Lesher, R. L., Oliger, A., Simpas, J. B., Brune, W. H., Schwab, J. J., Demerjian, K. L., He, Y., Zhou, X. L., and Gao, H. G.: OH and HO_2 chemistry in the urban atmosphere of New York City, Atmos. Environ., 37, 3639–3651, https://doi.org/10.1016/s1352-2310(03)00459-x, 2003.

Ren, X., Brune, W. H., Oliger, A., Metcalf, A. R., Simpas, J. B., Shirley, T., Schwab, J. J., Bai, C., Roychowdhury, U., Li, Y., Cai, C., Demerjian, K. L., He, Y., Zhou, X., Gao, H., and Hou, J.: OH, HO_2, and OH reactivity during the PMTACS-NY Whiteface Mountain 2002 campaign: Observations and model comparison, J. Geophys. Res.-Atmos., 111, D10S03, https://doi.org/10.1029/2005jd006126, 2006.

Ren, X., Sanders, J. E., Rajendran, A., Weber, R. J., Goldstein, A. H., Pusede, S. E., Browne, E. C., Min, K.-E., and Cohen, R. C.: A relaxed eddy accumulation system for measuring vertical fluxes of nitrous acid, Atmos. Meas. Tech., 4, 2093–2103, https://doi.org/10.5194/amt-4-2093-2011, 2011.

Ronen, R. and Galun, M.: Pigment extraction from lichens with dimethylsufoxide (DMSO) and estimation of chlorophyll degradation, Environ. Exp. Bot., 24, 239–245, https://doi.org/10.1016/0098-8472(84)90004-2, 1984.

Rummel, U., Ammann, C., Gut, A., Meixner, F. X., and Andreae, M. O.: Eddy covariance measurements of nitric oxide flux within an Amazonian rain forest, J. Geophys. Res.-Atmos., 107, LBA 17-11-LBA, 17–19, https://doi.org/10.1029/2001JD000520, 2002.

Sarwar, G., Roselle, S. J., Mathur, R., Appel, W., Dennis, R. L., and Vogel, B.: A comparison of CMAQ HONO predictions with observations from the Northeast Oxidant and Particle Study, Atmos. Environ., 42, 5760–5770, https://doi.org/10.1016/j.atmosenv.2007.12.065, 2008.

Scharko, N. K., Berke, A. E., and Raff, J. D.: Release of nitrous acid and nitrogen dioxide from nitrate photolysis in acidic

aqueous solutions, Environ. Sci. Technol., 48, 11991–12001, https://doi.org/10.1021/es503088x, 2014.

Šimek, M. and Cooper, J. E.: The influence of soil pH on denitrification: progress towards the understanding of this interaction over the last 50 years, Eur. J. Soil Sci., 53, 345–354, https://doi.org/10.1046/j.1365-2389.2002.00461.x, 2002.

Sörgel, M., Regelin, E., Bozem, H., Diesch, J.-M., Drewnick, F., Fischer, H., Harder, H., Held, A., Hosaynali-Beygi, Z., Martinez, M., and Zetzsch, C.: Quantification of the unknown HONO daytime source and its relation to NO_2, Atmos. Chem. Phys., 11, 10433–10447, https://doi.org/10.5194/acp-11-10433-2011, 2011a.

Ste-Marie, C. and Paré, D.: Soil, pH and N availability effects on net nitrification in the forest floors of a range of boreal forest stands, Soil Biol. Biochem., 31, 1579–1589, https://doi.org/10.1016/S0038-0717(99)00086-3, 1999.

Stemmler, K., Ammann, M., Donders, C., Kleffmann, J., and George, C.: Photosensitized reduction of nitrogen dioxide on humic acid as a source of nitrous acid, Nature, 440, 195–198, https://doi.org/10.1038/nature04603, 2006.

Stemmler, K., Ndour, M., Elshorbany, Y., Kleffmann, J., D'Anna, B., George, C., Bohn, B., and Ammann, M.: Light induced conversion of nitrogen dioxide into nitrous acid on submicron humic acid aerosol, Atmos. Chem. Phys., 7, 4237–4248, https://doi.org/10.5194/acp-7-4237-2007, 2007.

Strauss, S. L., Day, T. A., and Garcia-Pichel, F.: Nitrogen cycling in desert biological soil crusts across biogeographic regions in the Southwestern United States, Biogeochemistry, 108, 171–182, https://doi.org/10.1007/s10533-011-9587-x, 2012.

Stutz, J., Alicke, B., and Neftel, A.: Nitrous acid formation in the urban atmosphere: Gradient measurements of NO_2 and HONO over grass in Milan, Italy, J. Geophys. Res.-Atmos., 107, 8192, https://doi.org/10.1029/2001jd000390, 2002.

Su, H., Cheng, Y. F., Cheng, P., Zhang, Y. H., Dong, S., Zeng, L. M., Wang, X., Slanina, J., Shao, M., and Wiedensohler, A.: Observation of nighttime nitrous acid (HONO) formation at a non-urban site during PRIDE-PRD2004 in China, Atmos. Environ., 42, 6219–6232, https://doi.org/10.1016/j.atmosenv.2008.04.006, 2008a.

Su, H., Cheng, Y. F., Shao, M., Gao, D. F., Yu, Z. Y., Zeng, L. M., Slanina, J., Zhang, Y. H., and Wiedensohler, A.: Nitrous acid (HONO) and its daytime sources at a rural site during the 2004 PRIDE-PRD experiment in China, J. Geophys. Res.-Atmos., 113, D14312, https://doi.org/10.1029/2007jd009060, 2008b.

Su, H., Cheng, Y., Oswald, R., Behrendt, T., Trebs, I., Meixner, F. X., Andreae, M. O., Cheng, P., Zhang, Y., and Poeschl, U.: Soil nitrite as a source of atmospheric HONO and OH radicals, Science, 333, 1616–1618, https://doi.org/10.1126/science.1207687, 2011.

Tang, Y., An, J., Wang, F., Li, Y., Qu, Y., Chen, Y., and Lin, J.: Impacts of an unknown daytime HONO source on the mixing ratio and budget of HONO, and hydroxyl, hydroperoxyl, and organic peroxy radicals, in the coastal regions of China, Atmos. Chem. Phys., 15, 9381–9398, https://doi.org/10.5194/acp-15-9381-2015, 2015.

Tsai, C., Spolaor, M., Colosimo, S. F., Pikelnaya, O., Cheung, R., Williams, E., Gilman, J. B., Lerner, B. M., Zamora, R. J., Warneke, C., Roberts, J. M., Ahmadov, R., de Gouw, J., Bates, T., Quinn, P. K., and Stutz, J.: Nitrous acid formation in a snow-free wintertime polluted rural area, Atmos. Chem. Phys. Discuss., https://doi.org/10.5194/acp-2017-648, in review, 2017.

VandenBoer, T. C., Brown, S. S., Murphy, J. G., Keene, W. C., Young, C. J., Pszenny, A. A. P., Kim, S., Warneke, C., de Gouw, J. A., Maben, J. R., Wagner, N. L., Riedel, T. P., Thornton, J. A., Wolfe, D. E., Dubé, W. P., Öztürk, F., Brock, C. A., Grossberg, N., Lefer, B., Lerner, B., Middlebrook, A. M., and Roberts, J. M.: Understanding the role of the ground surface in HONO vertical structure: High resolution vertical profiles during NACHTT-11, J. Geophys. Res.-Atmos., 118, 10155–11171, https://doi.org/10.1002/jgrd.50721, 2013.

van Dijk, S. M., Gut, A., Kirkman, G. A., Gomes, B. M., Meixner, F. X., and Andreae, M. O.: Biogenic NO emissions from forest and pasture soils: Relating laboratory studies to field measurements, J. Geophys. Res.-Atmos., 107, LBA 25-21–LBA 25-11, https://doi.org/10.1029/2001JD000358, 2002.

Villena, G., Kleffmann, J., Kurtenbach, R., Wiesen, P., Lissi, E., Rubio, M. A., Croxatto, G., and Rappenglueck, B.: Vertical gradients of HONO, NO_x and O_3 in Santiago de Chile, Atmos. Environ., 45, 3867–3873, https://doi.org/10.1016/j.atmosenv.2011.01.073, 2011.

Vogel, B., Vogel, H., Kleffmann, J., and Kurtenbach, R.: Measured and simulated vertical profiles of nitrous acid – Part II. Model simulations and indications for a photolytic source, Atmos. Environ., 37, 2957–2966, https://doi.org/10.1016/s1352-2310(03)00243-7, 2003.

Wang, S. H., Ackermann, R., Spicer, C. W., Fast, J. D., Schmeling, M., and Stutz, J.: Atmospheric observations of enhanced NO_2-HONO conversion on mineral dust particles, Geophys. Res. Lett., 30, 1595, https://doi.org/10.1029/2003gl017014, 2003.

Weber, B., Wessels, D. C., Deutschewitz, K., Dojani, S., Reichenberger, H., and Büdel, B.: Ecological characterization of soil-inhabiting and hypolithic soil crusts within the Knersvlakte, South Africa, Ecological Processes, 2, 8, https://doi.org/10.1186/2192-1709-2-8, 2013.

Weber, B., Wu, D., Tamm, A., Ruckteschler, N., Rodriguez-Caballero, E., Steinkamp, J., Meusel, H., Elbert, W., Behrendt, T., Soergel, M., Cheng, Y., Crutzen, P. J., Su, H., and Pöschl, U.: Biological soil crusts accelerate the nitrogen cycle through large NO and HONO emissions in drylands, P. Natl. Acad. Sci. USA, 112, 15384–15389, https://doi.org/10.1073/pnas.1515818112, 2015.

Wong, K. W., Tsai, C., Lefer, B., Haman, C., Grossberg, N., Brune, W. H., Ren, X., Luke, W., and Stutz, J.: Daytime HONO vertical gradients during SHARP 2009 in Houston, TX, Atmos. Chem. Phys., 12, 635–652, https://doi.org/10.5194/acp-12-635-2012, 2012.

Wong, K. W., Tsai, C., Lefer, B., Grossberg, N., and Stutz, J.: Modeling of daytime HONO vertical gradients during SHARP 2009, Atmos. Chem. Phys., 13, 3587–3601, https://doi.org/10.5194/acp-13-3587-2013, 2013.

Wu, D., Kampf, C. J., Pöschl, U., Oswald, R., Cui, J., Ermel, M., Hu, C., Trebs, I., and Sörgel, M.: Novel tracer method to measure isotopic labeled gas-phase nitrous acid ($HO^{15}NO$) in Biogeochemical Studies, Environ. Sci. Technol., 48, 8021–8027, https://doi.org/10.1021/es501353x, 2014.

Yabushita, A., Enami, S., Sakamoto, Y., Kawasaki, M., Hoffmann, M. R., and Colussi, A. J.: Anion-catalyzed dissolution of NO_2

on aqueous microdroplets, J. Phys. Chem. A, 113, 4844–4848, https://doi.org/10.1021/jp900685f, 2009.

Young, C. J., Washenfelder, R. A., Roberts, J. M., Mielke, L. H., Osthoff, H. D., Tsai, C., Pikelnaya, O., Stutz, J., Veres, P. R., Cochran, A. K., VandenBoer, T. C., Flynn, J., Grossberg, N., Haman, C. L., Lefer, B., Stark, H., Graus, M., de Gouw, J., Gilman, J. B., Kuster, W. C., and Brown, S. S.: Vertically resolved measurements of nighttime radical reservoirs; in Los Angeles and their contribution to the urban uadical budget, Environ. Sci. Technol., 46, 10965–10973, https://doi.org/10.1021/es302206a, 2012.

Zhang, N., Zhou, X. L., Shepson, P. B., Gao, H. L., Alaghmand, M., and Stirm, B.: Aircraft measurement of HONO vertical profiles over a forested region, Geophys. Res. Lett., 36, L15820, https://doi.org/10.1029/2009gl038999, 2009.

Zhang, L., Wang, T., Zhang, Q., Zheng, J., Xu, Z., and Lv, M.: Potential sources of nitrous acid (HONO) and their impacts on ozone: A WRF-Chem study in a polluted subtropical region, J. Geophys. Res.-Atmos., 121, 3645–3662, https://doi.org/10.1002/2015JD024468, 2016.

Zhou, X. L., Gao, H. L., He, Y., Huang, G., Bertman, S. B., Civerolo, K., and Schwab, J.: Nitric acid photolysis on surfaces in low-NO_x environments: Significant atmospheric implications, Geophys. Res. Lett., 30, 2217, https://doi.org/10.1029/2003gl018620, 2003.

Zhou, X., Zhang, N., TerAvest, M., Tang, D., Hou, J., Bertman, S., Alaghmand, M., Shepson, P. B., Carroll, M. A., Griffith, S., Dusanter, S., and Stevens, P. S.: Nitric acid photolysis on forest canopy surface as a source for tropospheric nitrous acid, Nat. Geosci., 4, 440–443, https://doi.org/10.1038/ngeo1164, 2011.